Moments of the Longitudinal Proton Structure Function F_L from Global Data in the Q^2 Range 0.75–45.0 $(\mathrm{GeV}/c)^2$

P. Monaghan,[1] A. Accardi,[1,2] M. E. Christy,[1] C. E. Keppel,[1] W. Melnitchouk,[2] and L. Zhu[1]
[1]*Hampton University, Hampton, Virginia 23668, USA*
[2]*Jefferson Lab, Newport News, Virginia 23606, USA*
(Received 20 September 2012; published 9 April 2013)

We present an extraction of the lowest three moments of the proton longitudinal structure function F_L from world data between $Q^2 = 0.75$ and 45 $(\mathrm{GeV}/c)^2$. The availability of new F_L data at low Bjorken x from HERA and at large x from Jefferson Lab allows the first determination of these moments over a large Q^2 range, relatively free from uncertainties associated with extrapolations into unmeasured regions. The moments are found to be underestimated by leading twist structure function parametrizations, especially for the higher moments, suggesting either the presence of significant higher twist effects in F_L and/or a larger gluon distribution at high x.

DOI: 10.1103/PhysRevLett.110.152002 PACS numbers: 13.60.Hb, 12.38.Qk, 14.20.Dh

Introduction.—The suppression of the longitudinal deep-inelastic lepton-proton scattering cross section relative to the transverse cross section was an important early verification of the quarks' spin-1/2 nature. In fact, for a pointlike quark the longitudinal structure function F_L is zero. For a composite particle such as a proton, F_L is small but finite, and its exact value and momentum dependence reflect the quantum interaction effects between the proton's quark and gluon (or parton) constituents.

In QCD, one of the novel features of the proton longitudinal structure function is its strong sensitivity to the nonperturbative initial state distribution of gluons. The moments of F_L in particular are related to matrix elements of local twist-two operators, which can be computed directly in lattice QCD [1–3]. Traditionally, the gluon distribution $g(x)$ has been largely determined by studying the Q^2 evolution of the F_2 structure function, which at high photon virtualities is dominated by the transverse cross section. In recent global fits [4–9] $g(x)$ is further constrained at low parton momentum fraction x by jet production data in hadronic collisions.

At large values of x, where the cross sections are small, the extraction of the gluon density becomes increasingly difficult, leading to large uncertainties in $g(x)$ at $x \gtrsim 0.3$. As a result, the higher moments of F_L, which are weighted towards higher values of x, are particularly challenging to extract.

Data on F_L are generally difficult to extract from cross section measurements, requiring detailed longitudinal-transverse (L/T) separations in which experiments are performed at the same x and Q^2 but at different energy. Historically, the kinematic range spanned by F_L data was therefore rather limited, typically concentrated in the small- and intermediate-x regions, whereas a precise moment analysis necessitates a broad coverage in x at fixed Q^2. Previous moment analyses consequently required recourse to model-dependent estimates of the longitudinal to transverse structure function ratio [10], rendering a precise evaluation of F_L moments and their uncertainties problematic.

Recently, new data on the proton longitudinal structure function have been taken at low x from the H1 experiment [11] at HERA, and at large x from Hall C at Jefferson Lab [12,13]. The latter, in particular, cover a significant x range from $Q^2 = 4$ $(\mathrm{GeV}/c)^2$ down to $Q^2 < 1$ $(\mathrm{GeV}/c)^2$. Combined with the previous F_L results, the new data allow for the first time a direct extraction of the Q^2 dependence of several low F_L moments over a large range of Q^2.

In this Letter, we report the results of such an extraction, with an accurate determination of the lowest three moments of F_L, together with their uncertainties. Comparison of these to moments computed from parametrizations of leading twist parton distribution functions (PDFs) [4–6] then allows one to draw conclusions about the (poorly constrained) gluon distribution at large x, or the role of higher twist effects in the longitudinal cross section.

Data analysis.—Our analysis is performed in terms of the longitudinal Nachtmann moments, defined as [14]

$$M_L^{(n)}(Q^2) = \int_0^1 dx \frac{\xi^{n+1}}{x^3}\left\{F_L(x,Q^2) + 2(\rho^2-1) \times \frac{(n+1)/(1+\rho) - (n+2)}{(n+2)(n+3)} F_2(x,Q^2)\right\}, \quad (1)$$

where the Nachtmann scaling variable $\xi = 2x/(1+\rho)$, with $\rho = \sqrt{1+4M^2x^2/Q^2}$, and M is the proton mass [14,15]. The Nachtmann moments are constructed to remove from the data the kinematic dependence on the target mass [16–18], thus allowing a direct comparison with the Cornwall-Norton moments calculated from leading twist PDFs. At very low Q^2 this treatment may generate some residual uncertainty if the contributions from the threshold region at $\xi \to 1$ are large [19].

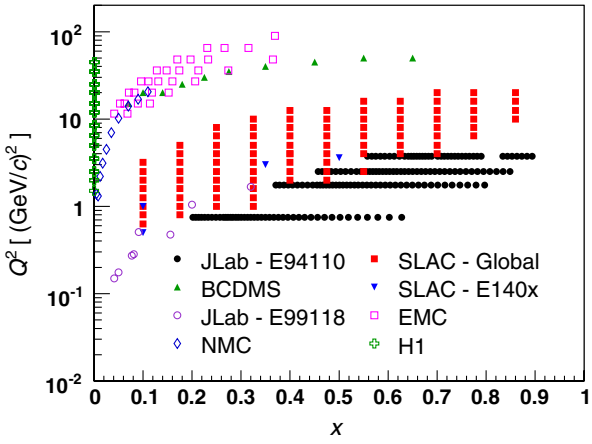

FIG. 1 (color online). The Q^2 and x distribution of F_L data sets used in this analysis. The new H1 data [11] at very small x appear clustered around the vertical axis because of the linear x scale.

In this analysis only F_L values extracted from dedicated, experimental L/T separations of the proton cross section data are used. This constraint is a critical requirement to avoid the introduction of model dependence into the $M_L^{(n)}$ extraction and to accurately estimate the uncertainties on the moments. The utilized proton F_L data come from a range of experiments at CERN (EMC [20], BCDMS [21], NMC [22]), SLAC (E140X [23], SLAC global [24]), DESY (H1 [11]), and Jefferson Lab (E94110 [12], E99118 [25]). The regions of the Q^2-x space covered by the data sets are shown in Fig. 1.

Since much of the data was not taken at fixed Q^2 values, the Q^2 bins were chosen to ensure the broad coverage in x necessary for a moment extraction. For instance, a typical bin at $Q^2 = 6.5$ (GeV/c)^2 included all data in the range of $6 < Q^2 < 7$ (GeV/c)^2. To account for any Q^2 dependence in the bin, the data were bin centered to the central Q^2 utilizing a combination of global data fits which gave good descriptions of the data over the relevant kinematic range. A sample of these data bin centered in Q^2 is shown for several central Q^2 values in Fig. 2. For the x integration, the data were then binned in x from 0.01 to 1, utilizing bins of width $\Delta x = 0.01$.

The data shown in Fig. 2 provide the most comprehensive kinematical coverage of F_L to date. However, some regions of x with sparse data remain, especially at larger Q^2. These gaps were filled by utilizing phenomenological fits to calculate the structure function at the center of any empty x bin. For data with $W^2 > 3.9$ (GeV/c)^2, a model obtained by a fit [26] to world data was used, while for $W^2 < 3.9$ (GeV/c)^2 a fit to the resonance region data was employed [27]. (These models were also used for the bin centering in Q^2, discussed above.)

The fit values of F_L were also renormalized bin by bin. For $x > 0.4$, where experimental data are abundant, the fit value was renormalized by the ratio of the fit to the

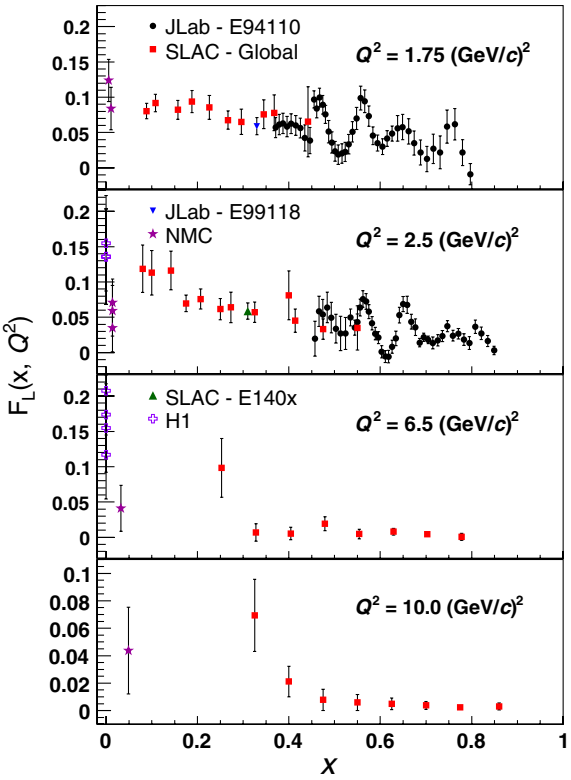

FIG. 2 (color online). Example plots of the F_L data used in this analysis for several Q^2 bins in the range 1.75–10.0 (GeV/c)^2.

error-weighted mean of the real data points at the start and end of each empty interval in x. For intervals with $x < 0.4$, where the x gaps are large and data scarce, the model was renormalized using the error-weighted mean of all real data points up to $x = 0.4$, to prevent a single data point at low x from biasing the renormalization factor.

Since the longitudinal Nachtmann moment defined in Eq. (1) includes contributions from both F_L and F_2, the entire analysis was repeated for the F_2 data of the same experiments. After filling the gaps in x for each Q^2 bin, each structure function was integrated as in Eq. (1) and the separate contributions were summed together to generate the longitudinal Nachtmann moments $M_L^{(n)}$ for $n = 2$, 4, and 6. The limits of integration were taken from $x = 0.01$ up to the inelastic or pion production threshold, $x_\pi = [1 + (m_\pi^2 + 2Mm_\pi)/Q^2]^{-1}$, with m_π the pion mass. Results with and without the elastic contribution included are presented below.

A Monte Carlo procedure was utilized to evaluate the errors on the moments. For each experimental F_2 and F_L data point, a Gaussian distribution with mean value and width equal to the value and total error of the data point was sampled to generate the pseudodata point at that x and Q^2 value. This resulted in a pseudodata set being generated for each Q^2 bin, and the procedure was repeated 1000 times. For each pseudodata set so generated, the x coverage gaps were filled using the method described above and the

data integrated to obtain 1000 pseudo-Nachtmann moments. The quoted value of the Nachtmann moment was then defined as the mean value of the pseudomoment distribution, and its statistical error as the distribution's standard deviation.

In order to estimate a model-dependent (systematic) error, the process of filling in the gaps in the data was repeated for three other combinations of models. The first two used the ALLM parametrization for F_2 [28,29] and the R1990 model for the longitudinal to transverse ratio [30] in the region with $W^2 > 3.9$ $(\mathrm{GeV}/c)^2$, in combination with two resonance region fits [27,31]. The third combination used the fit to world data from Ref. [26] for $W^2 > 3.9$ $(\mathrm{GeV}/c)^2$ and the resonance region [31] for lower W. After generating distributions of pseudomoments for all model combinations, the systematic error was defined as the maximum difference between the original model combination used to fill in the gaps and any of the other three combinations. The systematic error only has a significant contribution to the total error for the first two Q^2 bins of the $n = 2$ moment; otherwise, the statistical error dominates. Finally, the total error on each data point was calculated as the sum in quadrature of the statistical and systematic errors.

Results.—The extracted $n = 2$, 4, and 6 longitudinal Nachtmann moments are given in Table I, for Q^2 between 0.75 and 45 $(\mathrm{GeV}/c)^2$. The values include the measured inelastic contributions as well as the elastic component, computed from the global proton form factor parametrization in Ref. [32]. The elastic contribution is significant only for the lowest Q^2 bins, and decreases rapidly for $Q^2 \gtrsim 2$ $(\mathrm{GeV}/c)^2$. The errors are largely driven by the uncertainty on the F_L data.

TABLE I. The experimental longitudinal Nachtmann moments $M_L^{(n)}$ (scaled by 10^{-3}) extracted from the data along with their statistical errors. The inelastic results for the $n = 2$, 4, and 6 moments are given for each Q^2 bin, with the elastic (el) contribution shown only for the four lowest Q^2 bins.

Q^2	$M_L^{(n)} \times 10^{-3}$		
$(\mathrm{GeV}/c)^2$	$n = 2$	$n = 4$	$n = 6$
0.75(el)	12.4 ± 5.7	8.3 ± 1.9	3.64 ± 0.63
0.75	19.7 ± 3.3	1.2 ± 0.4	0.18 ± 0.08
1.75(el)	−1.6 ± 0.6	0.09 ± 0.28	0.31 ± 0.13
1.75	29.7 ± 2.4	2.8 ± 0.2	0.60 ± 0.07
2.5(el)	−1.0 ± 0.2	−0.23 ± 0.09	−0.03 ± 0.05
2.5	27.0 ± 4.7	2.9 ± 0.3	0.76 ± 0.07
3.75(el)	−0.4 ± 0.05	−0.14 ± 0.02	−0.06 ± 0.01
3.75	17.5 ± 7.7	1.6 ± 0.4	0.46 ± 0.08
5.0	16.3 ± 6.7	1.0 ± 0.7	0.26 ± 0.30
6.5	7.7 ± 6.3	0.6 ± 0.4	0.17 ± 0.12
8.0	24.7 ± 14.1	1.3 ± 0.5	0.26 ± 0.11
10.0	15.5 ± 8.8	0.9 ± 0.4	0.20 ± 0.10
15.0	2.7 ± 9.8	0.4 ± 0.6	0.13 ± 0.09
20.0	0.2 ± 9.1	−0.2 ± 0.8	0.01 ± 0.14
45.0	5.4 ± 11.0	0.2 ± 0.3	0.0 ± 0.05

The experimental Nachtmann moments are shown in Fig. 3 and compared with calculations of the Cornwall-Norton moments of F_L using the MSTW08 [4], ABKM09 [6], and CTEQ-Jefferson Lab (CJ) [5] global PDF parametrizations.

The MSTW08 fit included data on the F_2 and F_L structure functions in fixed target experiments and HERA collider data on reduced deep inelastic scattering (DIS) cross sections satisfying $Q^2 > 2$ $(\mathrm{GeV}/c)^2$ and $W^2 > 15$ $(\mathrm{GeV}/c)^2$. The kinematic cuts were imposed to avoid the region where higher twist (HT) effects may be significant, thereby excluding data at high x. Nuclear corrections in deuterium DIS were not included in the fit, although these strongly affect the d quark and gluon PDFs, even within the cuts used [33]. Jet data in pp collisions were also included, constraining the gluon PDF at $x \lesssim 0.3$.

For the CJ analysis [5], a similar data set to that used by MSTW08 was fitted, although F_L data were not directly included. The primary constraint here on the F_L structure function, and the large-x gluon PDF, was therefore from scaling violations in the F_2 data. Significantly, the kinematical cuts were relaxed to $Q^2 > 1.69$ $(\mathrm{GeV}/c)^2$ and $W^2 > 3$ $(\mathrm{GeV}/c)^2$, increasing considerably the large-x coverage afforded by the high-precision SLAC and Jefferson Lab data. The less restrictive cuts necessitated inclusion of target mass (TM) and HT contributions, as well as nuclear corrections [34,35]. The latter account for Fermi motion and binding of the nucleons, and were incorporated using both nonrelativistic (AV18, CD-Bonn, Paris) and relativistic (WJC) models of the deuteron [9]. Since the DIS data were limited to the F_2 structure function, only the leading twist contribution to $M_L^{(n)}$ could be computed from these PDFs.

The ABKM09 fit [6] used similar cuts to the CJ analysis, and also included nuclear, TM, and HT corrections, but did not utilize Jefferson Lab data. Fits were performed to DIS cross sections directly, rather than to the extracted F_2, although the exclusion of jet data from the analysis weakens the constraints on the gluon PDF at $x \lesssim 0.3$. Furthermore, HT terms were included for both F_2 and F_L, allowing calculation of moments up to twist 4.

Comparison of the measured moments with the PDF-based next-to-leading order (NLO) calculations in Fig. 3 (left) shows a turnover of the inelastic moments at $Q^2 \approx$ 2–3 $(\mathrm{GeV}/c)^2$. This is due to the effect of the pion threshold x_π, which decreases the limit of integration of the real data at low Q^2 values. At about the same Q^2 value, the elastic contribution also becomes non-negligible. Theoretical calculations of the DIS cross sections which neglect the pion threshold and integrate up to $x = 1$ can therefore be meaningfully compared to data only for $Q^2 \gtrsim 3$ $(\mathrm{GeV}/c)^2$.

The leading twist calculations are in generally good agreement with the data for $Q^2 \gtrsim 10$ $(\mathrm{GeV}/c)^2$. At lower

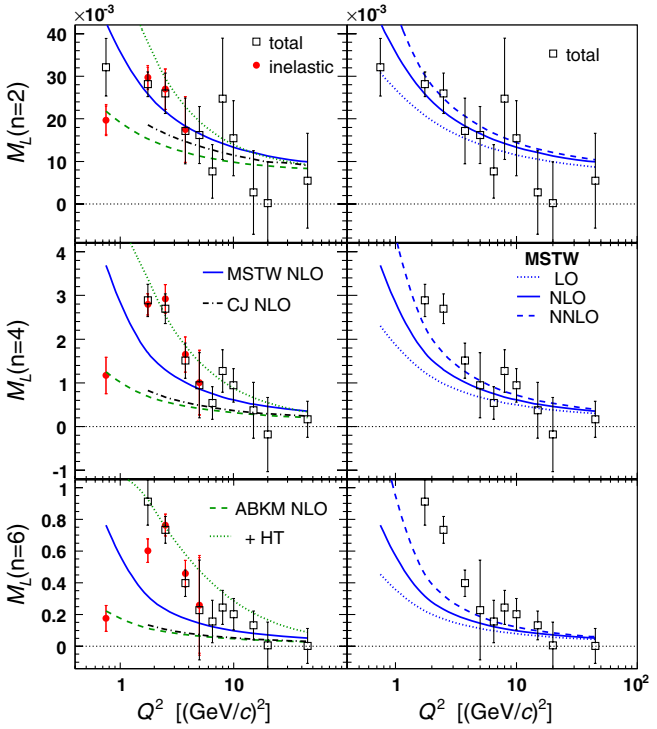

FIG. 3 (color online). Longitudinal Nachtmann moments $M_L^{(n)}$ for $n = 2$, 4 and 6, as a function of Q^2, for the measured inelastic (circles) and inelastic plus elastic (squares) contributions. The left-hand panels compare the data with calculations based on global NLO fits to PDFs from MSTW08 [4], ABKM09 [6] (including also HT corrections), and CJ [5], while the right-hand panels show the comparison with the MSTW08 fits for different orders in α_s (LO, NLO, and NNLO).

Q^2 the fits underestimate the data, particularly for the higher moments where large x plays an increasing important role. The disagreement with the low-Q^2, large-n data may reflect the poorly constrained gluon PDF, or possibly large effects from higher order perturbative QCD or higher twist corrections at large values of x.

The effect of including higher order terms is illustrated in Fig. 3 (right), where the total Nachtmann moments are compared with moments calculated from the MSTW08 PDFs [4] at leading order (LO), NLO, and next-to-next-to-leading order (NNLO). While the LO results generally underestimate the data at low Q^2, the agreement progressively improves with increasing order. It is only in the highest ($n = 6$) moment that any discrepancy appears, possibly indicating some underestimation of $g(x)$ at high x. There is a well-known and large uncertainty on $g(x)$ which can also be observed in the substantial differences in the NLO calculations from different PDFs, as shown in Fig. 3 (left).

The role of HT contributions in explaining the missing strength at small Q^2 can be explored by comparing the ABKM09 fit [6] with and without higher twist contributions. Inclusion of HT corrections improves the agreement with data, but overestimates the strength somewhat, even within the relatively large uncertainty of the HT contributions. This remains true even in the ABKM09 NNLO fit (not shown), where the LT contribution increases, albeit more slowly than in the MSTW08 fit, and the HT terms decrease, leaving the total curve stable. Since the ABKM09 fit does not include the recent Jefferson Lab data [25,36], it is not directly constrained at lower Q^2 and larger x. Minimizing extrapolation uncertainties and precisely studying the interplay of leading and higher twist contributions in this region will require use of the new data in global fits.

Conclusions.—In summary, we have extracted the lowest three Nachtmann moments of the proton longitudinal structure function over the range $Q^2 = 0.75$–45.0 $(\mathrm{GeV}/c)^2$ from world F_L data augmented by recent small-x measurements by the H1 Collaboration at HERA and large-x measurements from Jefferson Lab. Although the data coverage in x is not absolute, four different combinations of models have been used to fill gaps in the data, allowing the moments to be calculated with a rigorous uncertainty analysis. A reasonable estimate of the errors has been obtained by a statistical analysis of the moments calculated from a Monte Carlo procedure for sampling the data.

Comparison of the experimental moments with perturbative QCD calculations using recent global PDF fits reveals a need for either increased high-x gluon distribution, which is possible given its large uncertainty, or possibly non-negligible higher twist effects. Discrepancies between data and the PDFs increase as the moment order increases, but are reduced by increasing the order of perturbation theory. Neglecting higher twist terms or higher order calculations in the global fits may overestimate the extracted gluon distributions at large x, as shown by the comparison of ABKM09 and MSTW08 calculations.

Relatively good constraints on the large-x gluon can already be obtained from the scaling violations of F_2, provided that a weak cut on W is considered along with TM and HT included, as shown in the CJ fits [5]. However, inclusion of F_L data in global fits is required to provide direct constraints on the gluons, with the recent Jefferson Lab data at low $Q^2 < 4$ GeV^2, in particular, facilitating a considerable extension of reach in x.

We thank A. Psaker for his collaboration in the early stages of this work, and R. Ent for many informative discussions. This work was supported by the U.S. Department of Energy Contract No. DE-AC05-06OR23177, under which Jefferson Science Associates, LLC operates Jefferson Lab, and U.S. National Science Foundation Grant No. 1002644.

[1] Y. Aoki, T. Blum, H.-W. Lin, S. Ohta, S. Sasaki, R. Tweedie, J. Zanotti, and T. Yamazaki, Phys. Rev. D **82**, 014501 (2010).

[2] J. D. Bratt *et al.* (LHPC Collaboration), Phys. Rev. D **82**, 094502 (2010).

[3] D. Pleiter *et al.* (QCDSF/UKQCD Collaboration), Proc. Sci., LATTICE2010 (**2010**) 153.
[4] A. D. Martin, W. J. Stirling, R. S. Thorne, and G. Watt, Eur. Phys. J. C **63**, 189 (2009).
[5] A. Accardi, W. Melnitchouk, J. F. Owens, M. E. Christy, C. E. Keppel, L. Zhu, and J. G. Morfín, Phys. Rev. D **84**, 014008 (2011).
[6] S. Alekhin, J. Blümlein, S. Klein, and S. Moch, Phys. Rev. D **81**, 014032 (2010).
[7] R. D. Ball, V. Bertone, F. Cerutti, L. D. Debbio, S. Forte, A. Guffanti, J. I. Latorre, J. Rojo, and M. Ubiali, Nucl. Phys. **B855**, 153 (2012).
[8] P. Jimenez-Delgado and E. Reya, Phys. Rev. D **79**, 074023 (2009).
[9] J. F. Owens, A. Accardi, and W. Melnitchouk, arXiv:1212.1702.
[10] G. Ricco, S. Simula, and M. Battaglieri, Nucl. Phys. **B555**, 306 (1999).
[11] F. Aaron *et al.*, Eur. Phys. J. C **71**, 1579 (2011).
[12] Y. Liang *et al.*, arXiv:nucl-ex/0410027.
[13] Resonance Data Archive, https://hallcweb.jlab.org/resdata/.
[14] O. Nachtmann, Nucl. Phys. **B63**, 237 (1973).
[15] O. W. Greenberg and D. Bhaumik, Phys. Rev. D **4**, 2048 (1971).
[16] I. Schienbein *et al.*, J. Phys. G **35**, 053101 (2008).
[17] L. T. Brady, A. Accardi, T. J. Hobbs, and W. Melnitchouk, Phys. Rev. D **84**, 074008 (2011).
[18] H. Georgi and H. D. Politzer, Phys. Rev. D **14**, 1829 (1976).
[19] F. M. Steffens and W. Melnitchouk, Phys. Rev. C **73**, 055202 (2006).
[20] J. Aubert *et al.*, Nucl. Phys. **B259**, 189 (1985).
[21] A. Benvenuti *et al.*, Phys. Lett. B **237**, 592 (1990).
[22] M. Arneodo *et al.*, Nucl. Phys. **B483**, 3 (1997).
[23] L. H. Tao *et al.* (E140X Collaboration), Z. Phys. C **70**, 387 (1996).
[24] L. W. Whitlow, E. M. Riordan, S. Dasu, S. Rock, and A. Bodek, Phys. Lett. B **282**, 475 (1992).
[25] V. Tvaskis *et al.*, Phys. Rev. Lett. **98**, 142301 (2007).
[26] M. E. Christy, J. Blümlein, and H. Böttcher, arXiv:1201.0576.
[27] Y. Liang, Ph.D. thesis, The American University, 2003.
[28] H. Abramowicz and A. Levy, arXiv:hep-ph/9712415.
[29] H. Abramowicz, E. Levin, A. Levy, and U. Maor, Phys. Lett. B **269**, 465 (1991).
[30] L. W. Whitlow, Ph. D. thesis, Stanford University [SLAC Report No. SLAC-0357, 1990].
[31] M. E. Christy and P. E. Bosted, Phys. Rev. C **81**, 055213 (2010).
[32] J. Arrington, W. Melnitchouk, and J. A. Tjon, Phys. Rev. C **76**, 035205 (2007).
[33] A. Accardi, M. E. Christy, C. E. Keppel, W. Melnitchouk, P. Monaghan, J. G. Morfín, and J. F. Owens, Phys. Rev. D **81**, 034016 (2010).
[34] S. A. Kulagin and R. Petti, Nucl. Phys. **A765**, 126 (2006).
[35] Y. Kahn, W. Melnitchouk, and S. A. Kulagin, Phys. Rev. C **79**, 035205 (2009).
[36] M. E. Christy *et al.*, Phys. Rev. C **70**, 015206 (2004).